Photoluminescence Studies of Wurtzite Type W-ZnAl$_2$S$_4$ Single Crystals

Tetsuya KAI[*1], Masakazu KAIFUKU, Igor AKSENOV and Katsuaki SATO[*2]

Faculty of Technology, Tokyo University of Agriculture and Technology, Koganei, Tokyo 184, Japan

Single crystals of wurtzite-type W-ZnAl$_2$S$_4$ have been grown by the chemical vapor transport technique. Structural studies of the obtained crystals using powder X-ray diffraction analysis revealed their wurtzite structure with random distribution of cations at tetrahedral sites, whereas optical experiments showed that the crystals obtained had a direct band gap of $\sim$3.7 eV and exhibited a strong blue photoluminescence (PL) even at room temperature, with two different luminescence peaks, each of which had a different excitation band. In order to explain the PL results, the configuration coordinate model for the radiative transitions involved in the formation of the PL bands has been proposed. The model takes into account a lattice relaxation around the deep center responsible for the blue emissions, as well as the splitting of the valence band of W-ZnAl$_2$S$_4$ caused by the effect of the noncubic crystal field and spin-orbit interaction.

KEYWORDS: ZnAl$_2$S$_4$, wurtzite type structure, photoluminescence, blue emission

1. Introduction

The novel defective ternary compound ZnAl$_2$S$_4$ is recently attracting much interest due to its high photoconductivity[1] and promising energy band gap which is expected to be in the ultraviolet spectral region.[2] Therefore, this material can be considered as a prospective candidate for blue light-emitting device application. Since ZnAl$_2$S$_4$ is an defective compound, it crystallizes in several crystal structures depending on the conditions of material preparation, such as the temperature of compound synthesis and the Al/Zn ratio.[3-7] In the low-temperature region (800–900°C), ZnAl$_2$S$_4$ exists in two structures, i.e., a defect spinel phase α and a wurtzite phase W, while at higher temperatures (1050–1100°C) an orthorhombic phase β (which is an ordered version of the W-phase) and a rhombohedral phase γ coexist with the W-phase.

Although the structural properties of ZnAl$_2$S$_4$ are fairly well established, and there have been a few reports on the IR absorption[8] and optical absorption and Raman scattering[9] in α-ZnAl$_2$S$_4$, as well as on IR absorption in the γ-phase of this compound,[5] no optical study of W-ZnAl$_2$S$_4$ has been reported, causing the complete absence of any information on the optical and defect properties of this material.

In addition, ZnAl$_2$S$_4$ has been found to be involved in the strong blue emission in heavily Zn-doped CuAlS$_2$, in which phase separation into ZnAl alloy, ZnAl$_2$S$_4$ and CuAlS$_2$ was observed.[10]

Therefore, it is very important from the fundamental point of view, as well as for clarifying the origin of the blue emission from Zn-doped CuAlS$_2$, to investigate the optical (including photoluminescence) properties of W-ZnAl$_2$S$_4$.

In the present paper we report the results of the growth of ZnAl$_2$S$_4$ crystals by chemical vapor transport, as well as those of the structural and optical studies of the crystals obtained. The crystals of W-ZnAl$_2$S$_4$ have been studied using optical absorption, photoluminescence (PL) and photoluminescence excitation (PLE), as well as time-resolved PL techniques.

2. Experimental

ZnAl$_2$S$_4$ single crystals of the W- and β-phases were grown by the chemical vapor transport (CVT) technique from a powder of the α-ZnAl$_2$S$_4$ polycrystals as a starting material with iodine added as a transport agent. The polycrystals, also containing some mixture of the Al$_2$S$_3$ phase, had been prepared by heating the constituent elements (Zn, Al, and S of 99.999–99.9999% purity) in a BN crucible in a sealed quartz ampoule at 1250°C. The powder (obtained by crushing the polycrystals) was sealed in a quartz ampoule with iodine at the concentration of 10 mg/cm^3 of inner volume of the ampoule. CVT was carried out for 7 days with the temperatures of the charge zone and growth zone set at 780°C and 700°C, respectively. The resulting ZnAl$_2$S$_4$ crystals were found to be in two forms, i.e., a dominant single-crystalline form (W-phase) with dimensions of about $1 \times 1 \times 1$ mm^3, and a polycrystalline form (β-phase).[1] The single crystals were found to be transparent and colorless with pronounced twinning, as well as highly insulating, which precluded any study of their electrical properties. Similar properties were found for the polycrystals, except that they were colored slightly grey.

The crystal structures were evaluated by powder X-ray diffraction (XRD) using a Rigaku RAD IIC diffractometer. Absorption spectra were measured from crystals polished to the thickness of 80 μm at room temperature (RT) using a Hitachi U–3410 spectrophotometer. Static photoluminescence (PL) spectra were taken in the temperature range of 70–300 K using the 325 nm line of a Kimmon Electric CD3101R-1M He-Cd laser (10 mW) as an excitation source, a JASCO CT-25C monochromator, and Hamamatsu R928 photomultiplier. Time resolved PL spectra were measured using the 337-nm line of a Laser Science VSL-337 N$_2$ pulse laser and a Princeton Applied Research 4420 boxcar integrator. Photoluminescence excitation (PLE) spectra were taken using a Xe lamp combined with a JASCO CT-25A monochromator as an excitation source, the emitted light being

dispersed again by the JASCO CT-25C monochromator and detected by the photomultiplier.

3. Results and Discussion

3.1 Structural studies

Typical XRD patterns in the polycrystalline samples and single crystals of $ZnAl_2S_4$, obtained by the CVT method, are shown in Figs. 1 and 2, respectively. Since the pattern in the polycrystalline samples shows a complete correspondence to that in the orthorhombic modification of β-$ZnAl_2S_4$,[3] the polycrystalline samples can be regarded as having a wurtzite-derivative structure, in which S atoms are arranged in hexagonal close packing, whereas Zn and Al atoms are distributed in an orderly manner among tetrahedral sites.

On the other hand, the XRD pattern of the single-crystalline sample is very similar to the one reported in the wurtzite (W)-phase of $ZnAl_2S_4$,[6] except for several additional minor peaks of small intensity, which were not observed previously. In order to clear up this contradiction we have performed computer calculations of the diffraction pattern for W-$ZnAl_2S_4$, with the results being shown in Fig. 3. The results of the calculations are found to be in a perfect agreement with the experimental ones, shown in Fig. 2. We, hence, believe that the single-crystalline $ZnAl_2S_4$ samples crystallize in the wurtzite-derivative structure with random distribution of cations among one available set of the possible tetrahedral sites. The above said absence of several minor peaks in the pattern of W-$ZnAl_2S_4$, reported by Hahn et al.,[6] is believed to be caused by the low sensitivity of the powder X-ray camera (non-focusing camera) used
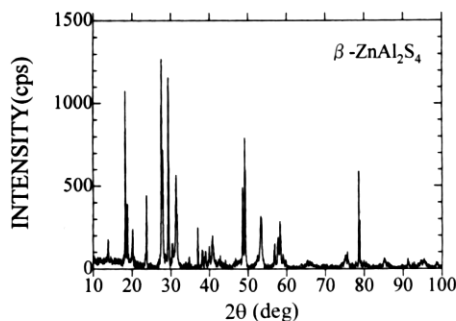
in the previous studies. Preliminary studies of the XRD analysis using the four-circle goniometer (Rigaku Rasa 5R II) revealed that the size of the unit cell (hexagonal: $a = 3.76$, $c = 6.15$ Å) is half that of the β-phase, supporting the above-mentioned assignment.

3.2 Optical properties

The typical optical absorption spectrum of the W-$ZnAl_2S_4$ single crystal is shown in Fig. 4. The absorption coefficient spectrum was calculated using transmission and absorption spectra. The dependence of the absorption coefficient α on the photon energy $h\nu$ has been found to satisfy the relation

$$\alpha(h\nu) = \frac{A}{h\nu}(h\nu - E_g)^{1/2} \tag{1}$$

where E_g is the band-gap energy and A is a constant. This result indicates that the fundamental edge of W-$ZnAl_2S_4$ is due to direct allowed transitions between nearly parabolic bands.[11] The band-gap energy of the compound under consideration has been estimated from the absorption spectra as 3.7 eV at RT. As can be seen from Fig. 4, the absorption spectrum is sharp, which indicates a low density of crystal defects in our samples.

Steady-state PL spectra in the polycrystalline β-$ZnAl_2S_4$ have been found to exhibit broad and weak yellow emission under ultraviolet (UV) excitation. Since no blue emissions were observed, it is considered that β-

Fig. 1. X-ray diffraction pattern for the polycrystalline $ZnAl_2S_4$ (β-phase).
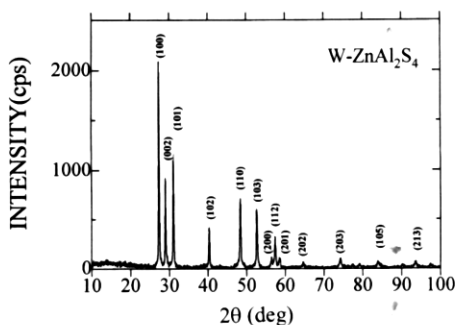
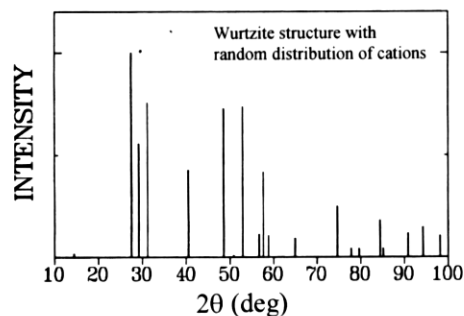Fig. 2. X-ray diffraction pattern for the single-crystalline $ZnAl_2S_4$ (W-phase).

Fig. 3. The calculated X-ray diffraction pattern for the wurtzite structure with random distribution of cations.
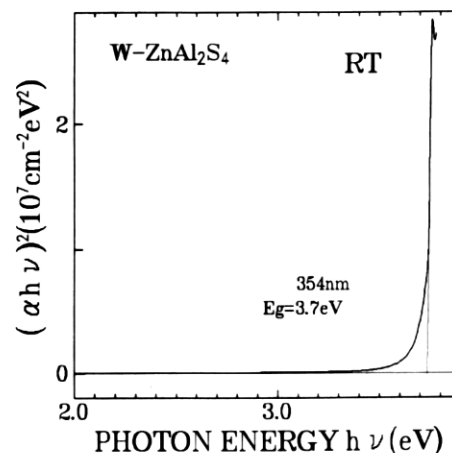

Fig. 4. The typical absorption spectrum of the single crystals of W-$ZnAl_2S_4$.

$ZnAl_2S_4$ is of no interest either for realizing the blue LED or for elucidating the nature of the intense blue emissions in the Zn-doped $CuAlS_2$ compound found in our previous studies.[10]

However, strong blue emission was observed under UV excitation by the 325-nm line of the He-Cd laser from the W-phase $ZnAl_2S_4$ single crystals, which is shown in Fig. 5. The peak of the blue emission has been found to shift with temperature from 450 nm at 70 K to about 480 nm at RT, the spectral position of the blue emission being close to that of the blue "self-activated" emission in $ZnS:Al$[12] and the blue emission observed by us in $CuAlS_2:Zn$.[10] The temperature-quenching curve of the blue emission, shown in the inset of Fig. 5, reveals a slope of about 120 meV which, however, does not correspond to the activation energy of any energy level in the band gap since the blue emission has been found to consist of two superposed emission bands, as discussed below. The blue emission was found to be visible for about 30 min after cutting off the optical excitation; this phosphorescence phenomenon was also observed in both $ZnS:Al$ and $CuAlS_2:Zn$.

The time-resolved spectra of the W-$ZnAl_2S_4$ crystals, taken at 70 K and RT, are shown in Figs. 6 and 7, respectively. It can be seen from these figures that, while no shift of the blue emission peak at 450 nm with time after excitation was observed at 70 K, the same emission measured at RT showed a shift of its peak position from 450 nm to 480 nm, the latter being the position of the peak of this emission in the static PL spectra taken at RT (see Figs. 5 and 7).

These results imply that 1) the blue luminescence does not originate from donor-acceptor pair radiative recombination, and 2) at RT the experimentally-observed emission is composed of two emissions, peaked at 450 and 480 nm, respectively, with energy transfer from the former emission to the latter one taking place as the time lapse after excitation.

At 70 K, PL peak position showed a strong dependence on the excitation energy. In order to clarify the origin of the peak shift, the PLE spectrum for the blue luminescence was measured at 70 K and the results are
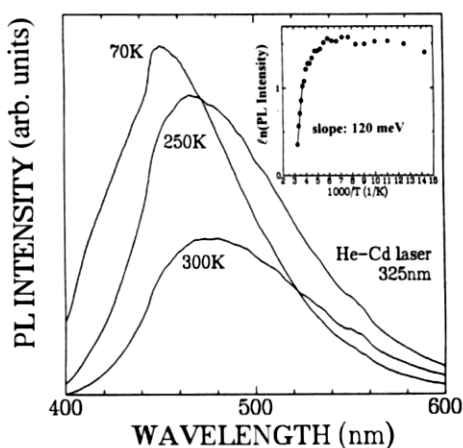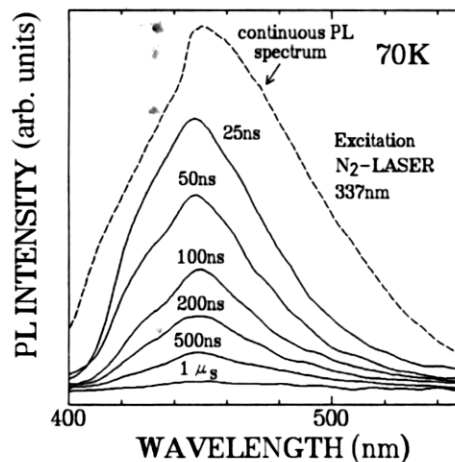

Fig. 6.   The time-resolved PL spectra of W-$ZnAl_2S_4$ taken at 70 K, together with the steady-state spectrum.
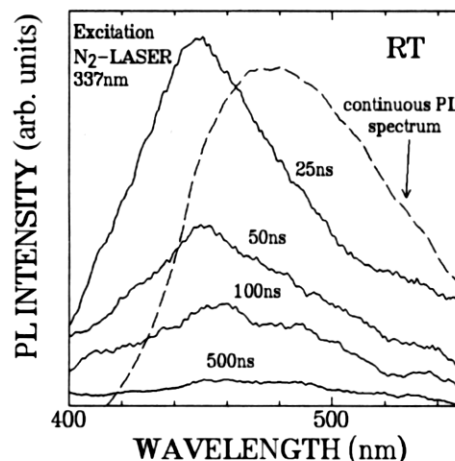

Fig. 7.   The time-resolved PL spectra of W-$ZnAl_2S_4$ taken at RT, together with the steady-state spectrum.
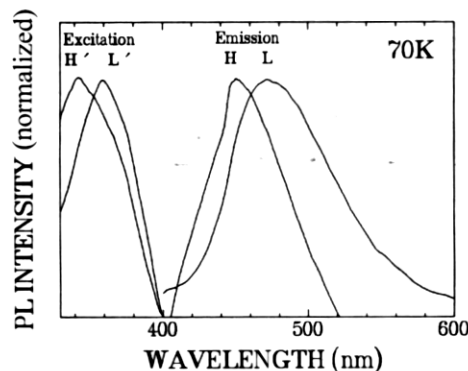

Fig. 8.   The PL spectra (H- and L-bands) and corresponding PLE (H'- and L'-bands) spectra measured at 70 K.

Fig. 5.   PL spectra of W-$ZnAl_2S_4$ taken at various temperatures under continuous UV excitation, with the thermal quenching curve for the luminescence shown in the inset.

shown in Fig. 8. For the wavelength of the detector-side monochromator longer than 476 nm (i.e., photon energies below 2.6 eV), the peak of the PLE spectrum was found at 360 nm (3.44 eV), denoted by L' in the figure, regardless of the detection energy, whereas for detection wavelength shorter than 443 nm (energies higher than

2.8 eV), the PLE peak remained at 340 nm (3.6 eV), denoted by H'. For emission wavelengths between 440 nm and 480 nm, the PLE peak apparently shifted between 340 nm and 360 nm. Therefore, it is clear that there are two distinct PLE bands. Corresponding to these two excitation peaks H' and L', different emission spectra with peaks H (~450 nm) and L (~480 nm) were observed, respectively, as shown in Fig. 8.

The method and the results obtained are similar to those reported for two red PL bands in the ternary compound $CuAlSe_2$, which were interpreted as radiative transitions from a deep donor center to the valence subbands of Γ_6- and Γ_7-symmetries, which were split from the uppermost Γ_{15} valence band of the chalcopyrite structure by the combined effect of the tetragonal crystal field and spin-orbit interaction.[13,14] The configuration coordinate model, taking into account the lattice relaxation around the deep donor center, has been proposed in order to explain the experimental results for these two red emissions in $CuAlSe_2$.[14] A similar model for the blue emissions from $W-ZnAl_2S_4$ is discussed below.

3.3   Proposed model for the radiative transitions

Let us consider the configuration coordinate model for a deep center, shown in Fig. 9, where Q is the crystal lattice distortion coordinate appropriate to the Jahn-Teller relaxation of a deep center due to the lowering of its symmetry as a result of electron capture, and $E(Q)$ is the potential energy. From the group-theory considerations, the valence band of $W-ZnAl_2S_4$ (wurtzite-type structure) in the center of the Brillouin zone is expected to be split into at least two subbands by the effect of the noncubic crystal field combined with the spin-orbit interaction. Hence, we can draw two lines, corresponding to the A- and B-valence subbands, for each of the

Fig. 9. Configuration coordinate model for the H- and L-emissions, where Q is the lattice distortion coordinate and $E(Q)$ is the potential energy.

excited states on the configuration coordinate scheme of Fig. 9. Excited state I corresponds to a free electron in the conduction band (CB) and a free hole in the valence band (VB), which the situation occurring immediately after optical band-to-band excitation. Excited state II corresponds to the case in which an electron (or a hole) is localized (trapped by the deep center), whereas a hole (or an electron) is free to move translationally in the VB (or CB). This is the situation occurring after some post-excitation time period, which is necessary for the deep center to trap the electron from the CB. The important point of the proposed configuration coordinate model is that at $Q = 0$, the energy lines of excited state I cross those of excited state II. Assuming, on the basis of the energy difference between the experimentally observed spectral positions of the H- and L-emissions and their respective excitation bands, that the energy for splitting of the VB is about 0.2 eV, our results on the blue emissions from $W-ZnAl_2S_4$ can be explained as follows.

At low temperature, the absorption of a photon with the energy of about 3.6 eV (H'-excitation) by the crystal results in a free electron (f.e.) in the CB and a free hole (f.h.) in the valence band at $Q = 0$, which corresponds to the adiabatic (vertical) photoabsorption process. On the configuration coordinate diagram, this photoabsorption corresponds to the transition from the ground state of the system to the excited state BI (Fig. 9). The following process is the trapping of the free electron by the deep center with the subsequent lattice relaxation around this center ($\Delta Q \neq 0$), and the system is converted from excited state BI to excited state BII. The following radiative recombination of this electron with the free hole in the VB results in the H-emission peak at 2.8 eV (450 nm).

Similarly (at low temperature) the absorption of the photon with the energy of about 3.4 eV (L'-excitation) results in the formation of excited state AI, with the subsequent relaxation of this state to excited state AII where the radiative recombination results in the L-emission at 2.6 eV.

We, therefore, experimentally observe two emission bands, spectrally separated by about 0.2 eV, each of which has its own excitation spectrum (Fig. 8). Since we observe two separate emission bands, we believe that the intervalence-band scattering time for the free holes is longer compared with the time required for the deep center to trap the free electron, which is proved by an absence of any shift of the H-emission peak with the time after excitation at low temperature (Fig. 6).

The situation, however, changes drastically as we increase the temperature, due to the thermally induced increase in the density of local vibrational modes and phonons. Upon increase of the temperature of the crystal lattice, the interaction of the holes in both A- and B-valence bands with the local and extended vibrational modes is enhanced. On the configuration coordinate diagram, this enhancement can be viewed as an increase in the number of holes occupying higher energy levels of the vibrational modes, and, hence, as an increase in the effective energy of excited state II.

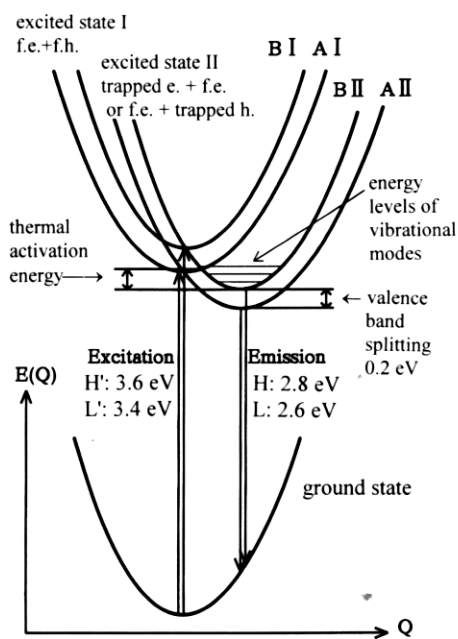Therefore, upon the increase of temperature, a greater

number of holes will have sufficient energy to overcome the potential barrier between the BII state and the AI state of the system, which results in the thermal quenching of H-emission with activation energy higher than that deduced from the thermal quenching curve ($\sim$0.12 eV) shown in the inset of Fig. 5. Moreover, since the holes, which have already overcome the potential barrier between the BII and AI states, will subsequently relax to the bottom of the AII state, we experimentally observe the shift of the emission from 450 nm (H-emission) to 480 nm (L-emission) upon the increase of temperature (Fig. 5).

The RT time-resolved spectra (Fig. 7) also support the above considerations. Since a finite time is required for the hole to accumulate enough energy via interaction with the vibrational modes to overcome the potential barrier between the BII and AI states, the longer the time period after excitation, the greater the number of holes will be able to transfer to the AI and, subsequently, to the AII state. The resulting emission, therefore, is expected to undergo the shift from the spectral position of the H-emission to that of the L-emission with time after excitation, which has been observed experimentally (Fig. 7).

We therefore believe that the configuration coordinate model proposed in this study qualitatively explains all the essential features of the blue emission from W-$ZnAl_2S_4$.

4. Conclusions

Single crystals of $ZnAl_2S_4$ compound having the wurtzite structure have been found to have the direct band gap of $\sim$3.7 eV and to exhibit two strong PL emissions in the blue spectral region, originating from the recombination of electrons trapped in the deep donor center with free holes occupying the two uppermost valence subbands, which are split from the valence band by the combined effect of the noncubic crystal field and spin-orbit interaction. The proposed configuration coordinate model of the radiative transitions, taking into account the Jahn-Teller relaxation of the crystal lattice around the emission center, explains all the main features of the blue emission.

Further investigations are required to clarify the origin of the deep center involved in the emission. It is of interest to study the microstructure of this presumably complex defect by a method of optically-detected magnetic resonance (ODMR). Such a study is planned for the near future.

1) S. I. Radautsan and I. M. Tiginyanu: *Proc. 9th Int. Conf. Ternary and Multinary Compounds, Yokohama, August 1993*, Jpn. J. Appl. Phys. **32** (1993) Suppl. 32-3, p. 5.
2) O. V. Kulikova, L. L. Kulyuk, N. A. Moldovyan, S. M. Popov, D. S. Remengo and A. V. Siminel: *Proc. 8th Int. Conf. Ternary and Multinary Compounds, Kishinev, September 1990*, (Moldavyan Acad. Sci., Kishinev, 1991) p. 353.
3) G. Steigmann: Acta Cryst. **23** (1967) 142.
4) S. Bonsall and F. Hummel: J. Solid State Chem. **25** (1978) 379.
5) M. Hills, D. Harris and C. Lowe-Ma: J. Phys. Chem. Solids **48** (1987) 501.
6) H. Hahn and G. Frank: Z. Anorg. Allg. Chem. **269** (1952) 227.
7) H. Berthold, K. Kohler and R. Wartchow: Z. Anorg. Allg. Chem. **496** (1983) 7.
8) H. Haeuseler and A. Canzis: Z. Naturforsch. B **38** (1983) 311.
9) O. Kulikova, N. Moldovyan, S. Popov, S. Radautsan and A. Siminel: *Proc. 9th Int. Conf. Ternary and Multinary Compounds, Yokohama, August 1993*, Jpn. J. Appl. Phys. **32** (1993) Suppl. 32-3, p. 586.
10) I. Aksenov, M. Matsui, T. Kai and K. Sato: Jpn. J. Appl. Phys. **32** (1993) 4542.
11) E. J. Johnson: Semicond. & Semimet. **3** (1967) 153.
12) K. Era, S. Shionoya and Y. Washizawa: Phys. Chem. Solids **29** (1968) 1827.
13) N. Yamamoto: Jpn. J. Appl. Phys. **15** (1976) 1909.
14) S. Chichibu, M. Shishikura, J. Ino and S. Matsumoto: J. Appl. Phys. **70** (1991) 1648.